

## Excited states of the negatively charged nitrogen-vacancy color center in diamond

Yuchen Ma,<sup>1,\*</sup> Michael Rohlfing,<sup>1</sup> and Adam Gali<sup>2</sup>

<sup>1</sup>*Fachbereich Physik, Universität Osnabrück, D-49069 Osnabrück, Germany*

<sup>2</sup>*Department of Atomic Physics, Budapest University of Technology and Economics, Budafoki út 8, H-1111 Budapest, Hungary*

(Received 5 January 2010; published 27 January 2010)

Excited states of the negatively charged nitrogen-vacancy color center in diamond are studied using *ab initio* many-body perturbation theory (within *GW* approximation and Bethe-Salpeter equation), including electronic exchange, correlation, and electron-hole interaction effects. We find that three singlets, one of which exhibits an intersystem crossing with the excited triplet, may be relevant for the fluorescence process in a way which has never been considered before. The calculated zero-phonon line for the visible excitation and that for the transition among the singlets are in good agreement with the experiments.

DOI: [10.1103/PhysRevB.81.041204](https://doi.org/10.1103/PhysRevB.81.041204)

PACS number(s): 61.72.jn, 71.35.Cc

Negatively charged nitrogen-vacancy (NV) center in diamond attracts a great deal of interest in recent years due to its extraordinary electronic and optical properties. The sharp zero-phonon line (ZPL) at 637 nm (Ref. 1) and the photostability at room temperature make the NV center a good candidate as the single photon source for quantum cryptography.<sup>2,3</sup> The NV center has a paramagnetic spin ground state whose spin can be optically polarized and readout, and also exhibits a long-lived spin coherence time at room temperature, which make it have important applications in quantum information processing and quantum computing.<sup>4-7</sup> Furthermore, the extremely high sensitivity of the electron spin of the NV center to the environment finds applications in nanoscale magnetic imaging.<sup>8,9</sup>

The knowledge of the electronic and spin structures of the NV center in the excited state, which provides upper limits on the fidelity of the cycling transition used for spin readout, is crucial for its future applications, particularly in quantum information technology. The excited-state structure of the defect is not yet fully understood, which hinders the understanding of the spin-flip fluorescence of the NV center. The general idea is that the spin polarization is initialized through intersystem crossing (ISC) between spin triplet states and singlet states [cf. Figs. 2 and 3(b)] induced by spin-orbit interaction.<sup>10</sup> The transition between the ground-state triplet  $^3A_2$  and the excited-state triplet  $^3E$  is responsible for the ZPL at 637 nm. Two models, a one-level model and a two-level model,<sup>10</sup> have been proposed concerning the singlets. In the one-level model, one singlet  $^1A_1$  is assumed to be close to  $^3E$ , while in the two-level model one singlet  $^1E$  is close to  $^3E$  and one singlet  $^1A_1$  is between the  $^1E$  and  $^3A_2$ . Recently, a very weak infrared-absorption (IR) line at 1.19 eV has been measured in the NV center that was associated with the transition between  $^1E$  and  $^1A_1$ , supporting the two-level model.<sup>11</sup> However, the relative position of the singlets and triplets could not be obtained from these experiments. Theoretical studies might improve the understanding of the excited states and their order. Until now, however, most investigations of the NV center have been limited to density-functional theory (DFT),<sup>12-14</sup> the ability of which to describe the excited states is questionable.

A quantitative discussion of the excitation at color centers requires a comprehensive approach to both geometric and

electronic degrees of freedom, including a systematic treatment of exchange and correlation which dominate the excited electronic states. In this Letter we employ *ab initio* many-body perturbation theory (MBPT),<sup>15,16</sup> a combination of the *GW* approximation (GWA) and the Bethe-Salpeter equation (BSE), to study the excited states of the NV center. Within MBPT, electronic exchange and correlation effects are described by the electron self-energy operator within Hedin's *GW* approximation, accompanied by solving the BSE of correlated electron-hole excitations. In the excited state, the excited electron feels the presence of the hole left behind as a result of the Coulomb interaction between them, so they cannot be treated separately but could instead be well described by two-particle Green's function which fulfills BSE.<sup>15</sup> Correspondingly, the wave function in the excited state, which should describe the motion of the correlated electron-hole pair, is not given by a simple product of electron and hole wave functions but requires a more general representation to account for energetic and spatial correlation between the two particles (for details see Ref. 16). Interrelation with the geometric structure of the defect, which is crucial to discuss the details of electronic excitations, will involve DFT and constrained DFT as well (see below).

The *GW*+BSE approach has become a standard procedure for optical excitations in many systems including clusters, molecules and crystals, and also applied to color centers in crystals, e.g., in LiCl (Refs. 17 and 18) and CaF<sub>2</sub>.<sup>19</sup> In our previous work on the color center in CaF<sub>2</sub>, the calculated absorption and emission energies by *GW*+BSE agree well with experiment within 0.1 eV.<sup>19</sup> This is within the general accuracy of MBPT ( $\sim 0.1$  eV for many systems), which is limited (among others) by the *GW* approximation of the self-energy operator. For bulk diamond, our *GW*+BSE approach predicts the band gap at 5.7 eV, the absorption edge at 7.5 eV and the sharp absorption peak at 12.1 eV, which agree within 0.15 eV with the experiments.<sup>20,21</sup>

For the NV center in diamond, in this Letter we will show that (i) there are three singlet levels between  $^3A_2$  and  $^3E$ :  $^1E'$  close to  $^3E$ ,  $^1A_1$  halfway, and  $^1E$  close to  $^3A_2$ ; (ii) intersystem crossing occurs between  $^1E'$  and  $^3E$  during relaxation of nuclear positions induced by the electronic excitation; and (iii) we could identify the IR ZPL as the  $^1E' \rightarrow ^1A_1$  transition.

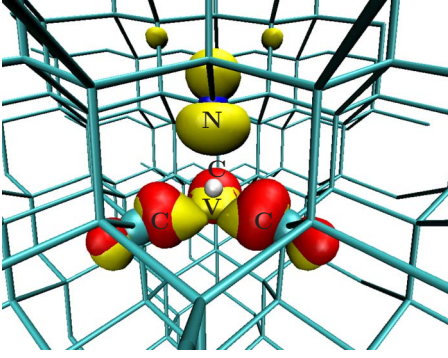


FIG. 1. (Color online) Real-space distribution of the excited electron (red/gray) and hole (yellow/light gray) in the excited state  ${}^3E$  of the NV center in diamond. N, C, and V denote the position of the nitrogen atom, the three-coordinated carbon atoms and the vacancy in the NV center, respectively.

Our findings change the previous models of the singlets, and we can clarify several aspects of the fluorescence of the NV center.

Throughout the paper (unless noted otherwise) we use a 256-atom body-centered cubic supercell which, according to our calculations, is large enough to achieve convergence in all relevant excitation energies. The ground-state calculation is performed within DFT by employing the PBE generalized gradient approximation and norm-conserving Troullier-Martins pseudopotentials. BSE is solved at the level of random-phase approximation instead of the Tamm-Dancoff approximation usually applied. The  $\Gamma$  point is used to represent the wave functions and operators in both DFT and  $GW+BSE$ , which is accurate enough for the large 256-atom supercell. We also consider the relaxation of nuclei induced by electronic excitation to calculate the ZPL. To map the potential-energy surface at the computationally very demanding  $GW+BSE$  level, we apply a 64-atom simple-cubic supercell which is too small for correct excitation energies, but large enough to monitor their dependence on the defect geometry.

The NV center consists of a substitutional nitrogen atom associated with a vacancy in an adjacent lattice site possessing  $C_{3v}$  symmetry (Fig. 1). The NV center has six electrons around the vacant site, four of them occupy the defect levels  $\nu$ ,  $\bar{\nu}$ ,  $e_x$ , and  $e_y$  in the band gap as shown in Fig. 2 (Ref. 13) and are involved in the optical process interested here, while the other two occupy the levels 1.2 eV below the valence-band maximum.<sup>13</sup> The orbitals  $\nu$  and  $e$  possess  $A_1$  and  $E$  symmetries, respectively. The  $|S, m_S\rangle = |1, 1\rangle$  ground state can be expressed by a single Slater determinant  $|\nu\bar{\nu}e_xe_y\rangle$ . The energies of the levels  $\bar{\nu}$ ,  $e_{x,y}$ , and the unoccupied  $\bar{e}_{x,y}$  relative to that of  $\nu$  are 0.6, 1.2, and 3.3 eV within GWA, respectively, with quasiparticle corrections of 0.2, 0.1, and 1.1 eV with respect to the DFT-PBE values, respectively. Description of the electronic exchange and correlation effects by a nonlocal and dynamical self-energy operator, instead of the local and static exchange-correlation functional usually used within DFT, makes GWA succeed in predicting the band gaps and band structures of semiconductors, insulators and metals with very good accuracy compared to experiments.<sup>15</sup>

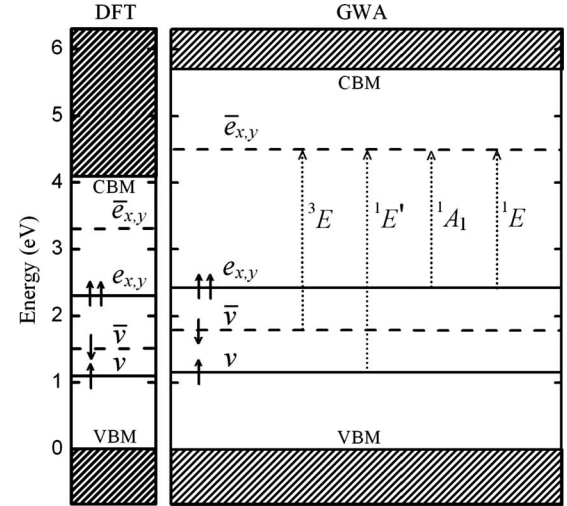


FIG. 2. The spin-polarized levels of the NV center in the ground state within DFT and GWA. The overbar in the wave function denotes down-spin electron. The valence-band maxima in both DFT and GWA are set to zero. CBM denotes the conduction-band minimum. Dotted arrows indicate excitations to the triplet and singlet excited states.

Accurate GWA calculation of the energy difference between different defect levels is a prerequisite for the BSE calculation in the next step.

With excitation, the down-spin electron in the orbital  $\bar{\nu}$  hops to  $\bar{e}_{x,y}$  as shown in Fig. 2, forming the spin triplet  ${}^3E$  with single Slater determinants  $|\nu e_x \bar{e}_x e_y\rangle$  or  $|\nu e_x e_y \bar{e}_y\rangle$  for  $|1, 1\rangle$ . We note that we leave a hole on the total symmetric  $\nu$  that is partially localized on the N atom, and place the electron on the  $e$  orbital with no localization on the N atom. Our calculated exciton wave function in Fig. 1 shows exactly this feature. Within the Franck-Condon principle, the absorption energy at the ground-state equilibrium structure (GES), illustrated as the line  $a \rightarrow b$  in Fig. 3(a), is calculated to be 2.32 eV. This is in good agreement with the experimental optical spectrum whose absorption sideband has its maximum around 2.2 eV.<sup>1</sup> The electron-hole pair is bound relatively weakly in this excited state, with a binding energy of about 0.3 eV, which makes the electron-hole wave function has a relatively large spatial distribution, about 1 nm as measured by the experiment.<sup>22</sup> The calculated radiative lifetime of  $\sim 10$  ns compares well with the experimental value of 12 ns.<sup>23,24</sup>

$GW+BSE$  yields three kinds of singlet excitations at energies of 0.40, 0.99, and 2.25 eV at GES, with twofold, one-fold and twofold degeneracy, respectively, between the triplet ground state ( $\equiv 0$  eV) and the  ${}^3E$  excitation at 2.32 eV. The configurations of the first two singlet states are  $\frac{1}{\sqrt{2}}[|\nu\bar{\nu}e_x\bar{e}_x\rangle - |\nu\bar{\nu}e_y\bar{e}_y\rangle]$  or  $\frac{1}{\sqrt{2}}[|\nu\bar{\nu}e_x\bar{e}_y\rangle + |\nu\bar{\nu}e_y\bar{e}_x\rangle]$  for the former and  $\frac{1}{\sqrt{2}}[|\nu\bar{\nu}e_x\bar{e}_x\rangle + |\nu\bar{\nu}e_y\bar{e}_y\rangle]$  for the latter, respectively, and can be ascribed to  ${}^1E$  (0.40 eV) and  ${}^1A_1$  (0.99 eV),<sup>11,25</sup> respectively. The third one, which is also a doublet with symmetry  $E$ , has never been reported before as an important state, and will be denoted as  ${}^1E'$  in the context. The states  ${}^1E'$  and  ${}^3E$  are nearly degenerated with the energy splitting smaller than 0.1 eV. The configuration of  ${}^1E'$  is  $|\bar{\nu}e_x\bar{e}_x e_y\rangle$  or

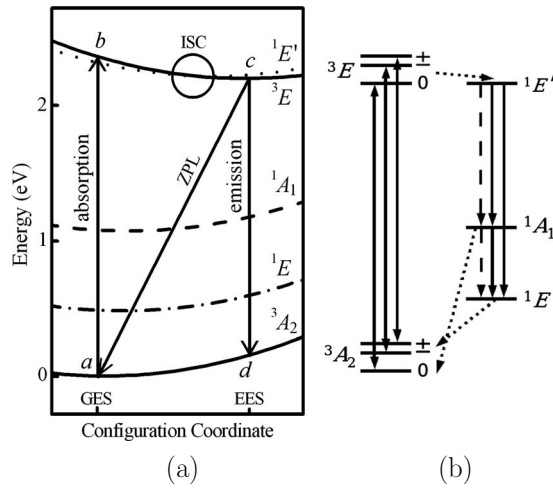


FIG. 3. (a) Energy profiles of the NV center within  $GW+BSE$  in the states  $^3A_2$ ,  $^1E$ ,  $^1A_1$ ,  $^3E$ , and  $^1E'$  along the CDFT relaxation path in the state  $^3E$ , respectively. ISC denotes the intersystem crossing between the states  $^3E$  and  $^1E'$ . (b) Simplified energy-level diagram for the NV center. The solid, dotted, and dashed lines indicate radiative transitions, intersystem crossing transitions, and vibronic decays, respectively.

$|\bar{\nu}e_x e_y \bar{e}_y\rangle$ , with the electron excited from the orbital  $\nu$  to  $\bar{e}_{x,y}$  involving a spin flip. The spatial distributions of the excited electron and hole in the state  $^1E'$  are similar to those in the state  $^3E$  as shown in Fig. 1 except for the different spin directions of the holes.

Calculation of ZPL needs to relax the NV center in the excited state, which is currently beyond the capability of  $GW+BSE$  due to the extremely huge computational cost. Instead, we utilize a simple approach which is a combination of constrained DFT (CDFT) and  $GW+BSE$ . First, CDFT, within which the occupancies in specific orbitals are fixed, is used to find the excited-state equilibrium structure (EES), and then the potential-energy surface in the excited state is evaluated by  $GW+BSE$ . This approach has succeeded in predicting the emission energy and Stokes shift of the color center in  $CaF_2$  with good accuracy (within 0.1 eV) compared to experiment.<sup>19</sup>

Starting from GES, through CDFT relaxation in the state  $^3E$ , employed by depopulating the level  $\bar{\nu}$  and populating the level  $\bar{e}_x$  or  $\bar{e}_y$ , the nitrogen atom moves toward the vacant center by 0.05 Å while the three undercoordinated carbon atoms move outwards by 0.06 Å. At EES, the positions of the levels  $e_{x,y}$  and  $\bar{e}_{x,y}$  remain nearly unchanged compared to those at GES, while the levels  $\nu$  and  $\bar{\nu}$  rise by 0.3 and 0.4 eV, respectively. By comparing the  $GW+BSE$  energy curve along the relaxation path from GES to EES with the CDFT energy curve, we find that the CDFT minimum is very close to the  $GW+BSE$  minimum, which proves the validity of our approach.<sup>19</sup> The energy profiles of the triplets and singlets within  $GW+BSE$  along the CDFT relaxation path are shown in Fig. 3(a). Here, for simplicity, we assume that in the singlets the NV center relaxes along the same path as that in the state  $^3E$ , which could be a good approximation due to the small displacements of the atoms between GES and EES.

The emission energy at EES calculated within Franck-

Condon approximation [line  $c \rightarrow d$  in Fig. 3(a)] is 1.95 eV, 0.15 eV higher than the energy of the experimental emission sideband maximum (1.80 eV).<sup>1</sup> The ZPL [line  $c \rightarrow a$  in Fig. 3(a)] is 2.09 eV which is also 0.15 eV higher than the experimental ZPL at 1.945 eV.<sup>1</sup> Generally, the agreement between  $GW+BSE$  and the experiment is good.

We find the  $^3E$  state above  $^1E'$  at GES, but at EES this order is inverted. About halfway in between, we find an ISC between the energy curves of these two states. Such ISC between the triplet and singlet states would play an important role in the spin-polarization process. As a consequence, instead of the commonly applied green light excitation, the yellow light excitation at the crossing point of  $^3E$  and  $^1E'$  states might enhance the spin-polarization effect of the NV center.

From Fig. 3(a), we can see that the energy curves of the states  $^1E$  and  $^1A_1$  are nearly parallel to each other. These two energy curves are also nearly parallel to the ground-state ( $^3A_2$ ) energy curve. This shows that the excitation energies of these two singlets are insensitive to the lattice relaxation, which is quite different from those of the states  $^3E$  and  $^1E'$ . The ZPL related to the transitions  $^1E' \rightarrow ^1A_1$ ,  $^1E' \rightarrow ^1E$ , and  $^1A_1 \rightarrow ^1E$  are 1.12, 1.71, and 0.59 eV, respectively.

Based on our calculations, the energy-level diagram of the NV center can be simply modeled by Fig. 3(b). Nonradiative transition from  $^3E$  to  $^1E'$  through ISC is the first step of the spin polarization in the optical cycle. In this process, little lattice rearrangement is expected since the spatial distribution of electrons in these two states is the same as discussed above. Only spin flip in the orbital  $\nu$  is involved during the transition. The closeness in energy between the states  $^3E$  and  $^1E'$  seems to agree with the experimental results by Dräbenstedt *et al.*<sup>26</sup> in which they interpreted their excitation spectrum as a singlet state about 37 meV below the  $^3E$  state. We have to mention that the typical accuracy of the  $GW+BSE$  approach is around 0.1 eV (see above), which is larger than the energy difference between the states  $^3E$  and  $^1E'$  ( $\sim 20$  meV). This, together with the fact that EES is obtained through CDFT instead of  $GW+BSE$ , do not allow us to draw final conclusions concerning the energy difference between these two states, their order and the existence and exact position of the crossing. However, the small energy gap between  $^3E$  and  $^1E'$ , as found in our calculation, would ensure a fast ISC rate. Several factors, e.g., strain commonly present in diamond,<sup>27</sup> external electric field and phonons, may split the energy levels, change the relative position of different levels and thus influence the ISC rate. Efficient ISC between  $^3E$  and  $^1E'$  gives the  $m_S = \pm 1$  sublevels in the state  $^3E$ , where ISC occurs, a shorter lifetime (7.8 ns) than the  $m_S = 0$  sublevel (12 ns).<sup>24</sup>

From  $^1E'$  the electron can decay to  $^1A_1$  or to  $^1E$ . We can associate the recently measured IR line at 1.19 eV (Ref. 11) with the  $^1E' \rightarrow ^1A_1$  transition (Table I). The strength of the radiative  $^1E' \rightarrow ^1A_1$  decay is about four order of magnitude smaller than the  $^3E \rightarrow ^3A_2$  emission.<sup>11</sup> Therefore, Rogers *et al.* claimed that the nonradiative process between these two singlets must be much faster. Our tools do not allow to prove this assumption. Our results indicate that the transition from  $^1A_1$  to  $^1E$ , whether radiative or nonradiative, is extraordinary weak. Otherwise, the system would decay to the  $m_S = \pm 1$

TABLE I. The calculated vertical absorption  $E_{\text{abs}}$  and emission  $E_{\text{emi}}$  energies and the zero-phonon lines within  $GW+BSE$  and their comparison with DFT results and experimental data.

	$E_{\text{abs}}$	$E_{\text{emi}}$	ZPL			
			${}^3E \rightarrow {}^3A_2$	${}^1E' \rightarrow {}^1A_1$	${}^1E' \rightarrow {}^1E$	${}^1A_1 \rightarrow {}^1E$
$GW+BSE$	2.32	1.95	2.09	1.12	1.71	0.59
DFT-PBE	1.87	1.51	1.68			
Expt.	2.20 <sup>a</sup>	1.80 <sup>a</sup>	1.945 <sup>a</sup>	1.19 <sup>b</sup>		

<sup>a</sup>Reference 1.

<sup>b</sup>Reference 11.

sublevels of the  ${}^3A_2$  state via  ${}^1E$ , which is in contradiction with the experiments. The nonradiative decay from  ${}^1A_1$  to the  $m_S=0$  sublevel in  ${}^3A_2$  should be a faster process but still relatively slow because of the large energy gap ( $\sim 1.0$  eV) between them. This explains the relatively long 300 ns lifetime of the “storage” singlet state.<sup>11,27</sup> As to the transition  ${}^1E' \rightarrow {}^1E$ , its ZPL is close that between the triplets within 0.4 eV, so the corresponding ZPL peak, if exist, may be merged into the emission sideband of the transition  ${}^3E \rightarrow {}^3A_2$  (Ref. 1) and cannot be discerned experimentally.

In summary, we have investigated the triplet and singlet states in the negative nitrogen-vacancy center in diamond within many-body perturbation theory. Three singlets are found between the triplets with the symmetry of  $E$ ,  $A_1$ , and

$E$ , respectively. The highest two singlets are responsible for the optically induced spin polarization and the ZPL related to the transition between them is comparable to the infrared emission among singlets observed in the experiment. Our results, especially the newly found singlet state close to the state  ${}^3E$ , provide insight into the optical process in the NV center of diamond and is important for the future application of NV center in quantum information technology.

This work has been supported by the Deutsche Forschungsgemeinschaft (Bonn, Germany) by Grant No. Ro 1318/4-3. A.G. would like to thank the support from Hungarian OTKA Grant No. K-67886 and Bolyai program from the Hungarian Academy of Sciences.

\*yuma@uos.de

<sup>1</sup>G. Davies and M. F. Hamer, Proc. R. Soc. London, Ser. A **348**, 285 (1976).

<sup>2</sup>A. Beveratos, R. Brouri, T. Gacoin, A. Villing, J. P. Poizat, and P. Grangier, Phys. Rev. Lett. **89**, 187901 (2002).

<sup>3</sup>C. Kurtsiefer, S. Mayer, P. Zarda, and H. Weinfurter, Phys. Rev. Lett. **85**, 290 (2000).

<sup>4</sup>M. V. G. Dutt, L. Childress, L. Jiang, E. Togan, J. Maze, F. Jelezko, A. S. Zibrov, P. R. Hemmer, and M. D. Lukin, Science **316**, 1312 (2007).

<sup>5</sup>L. Childress, M. V. G. Dutt, J. M. Taylor, A. S. Zibrov, F. Jelezko, J. Wrachtrup, P. R. Hemmer, and M. D. Lukin, Science **314**, 281 (2006).

<sup>6</sup>P. Neumann, N. Mizuochi, F. Rempp, P. Hemmer, H. Watanabe, S. Yamasaki, V. Jacques, T. Gaebel, F. Jelezko, and J. Wrachtrup, Science **320**, 1326 (2008).

<sup>7</sup>R. Hanson, V. V. Dobrovitski, A. E. Feiguin, O. Gywat, and D. D. Awschalom, Science **320**, 352 (2008).

<sup>8</sup>J. R. Maze *et al.*, Nature (London) **455**, 644 (2008).

<sup>9</sup>G. Balasubramanian *et al.*, Nature (London) **455**, 648 (2008).

<sup>10</sup>N. B. Manson and R. L. McMurtrie, J. Lumin. **127**, 98 (2007).

<sup>11</sup>L. J. Rogers, S. Armstrong, M. J. Sellars, and N. B. Manson, New J. Phys. **10**, 103024 (2008).

<sup>12</sup>F. M. Hossain, M. W. Doherty, H. F. Wilson, and L. C. L. Hollenberg, Phys. Rev. Lett. **101**, 226403 (2008).

<sup>13</sup>A. Gali, M. Fyta, and E. Kaxiras, Phys. Rev. B **77**, 155206 (2008).

<sup>14</sup>J. A. Larsson and P. Delaney, Phys. Rev. B **77**, 165201 (2008).

<sup>15</sup>G. Onida, L. Reining, and A. Rubio, Rev. Mod. Phys. **74**, 601 (2002).

<sup>16</sup>M. Rohlfing and S. G. Louie, Phys. Rev. B **62**, 4927 (2000).

<sup>17</sup>M. P. Surh, H. Chacham, and S. G. Louie, Phys. Rev. B **51**, 7464 (1995).

<sup>18</sup>M. L. Tiago and J. R. Chelikowsky, Phys. Rev. B **73**, 205334 (2006).

<sup>19</sup>Y. C. Ma and M. Rohlfing, Phys. Rev. B **77**, 115118 (2008).

<sup>20</sup>M. Rohlfing, P. Krüger, and J. Pollmann, Phys. Rev. B **48**, 17791 (1993).

<sup>21</sup>R. A. Roberts and W. C. Walker, Phys. Rev. **161**, 730 (1967).

<sup>22</sup>P. Tamarat *et al.*, Phys. Rev. Lett. **97**, 083002 (2006).

<sup>23</sup>A. T. Collins, M. F. Thomaz, and M. I. B. Jorge, J. Phys. C **16**, 2177 (1983).

<sup>24</sup>A. Batalov, C. Zierl, T. Gaebel, P. Neumann, I. Y. Chan, G. Balasubramanian, P. R. Hemmer, F. Jelezko, and J. Wrachtrup, Phys. Rev. Lett. **100**, 077401 (2008).

<sup>25</sup>A. Lenef and S. C. Rand, Phys. Rev. B **53**, 13441 (1996).

<sup>26</sup>A. Dräbenstedt, L. Fleury, C. Tietz, F. Jelezko, S. Kilin, A. Nizovtzev, and J. Wrachtrup, Phys. Rev. B **60**, 11503 (1999).

<sup>27</sup>N. B. Manson, J. P. Harrison, and M. J. Sellars, Phys. Rev. B **74**, 104303 (2006).